Wavelet-Based Representations for a Class of Self-Similar Signals with Application to Fractal Modulation

Gregory W. Wornell, *Member, IEEE,* and Alan V. Oppenheim, *Fellow, IEEE*

Abstract—**A potentially important family of self-similar signals is introduced based upon a deterministic scale-invariance characterization. These signals, which are referred to as "dy-homogeneous" signals because they generalize the well-known homogeneous functions, have highly convenient representations in terms of orthonormal wavelet bases. In particular, wavelet representations can be exploited to construct orthonormal "self-similar" bases for these signals. The spectral and fractal characteristics of dy-homogeneous signals make them appealing candidates for use in a number of applications. As one potential example, we consider their use in a communications-based context. Specifically, we develop a strategy for embedding information into a dy-homogeneous waveform on multiple time-scales. This multirate modulation strategy, which we term "fractal modulation," is potentially well-suited for use with noisy channels of simultaneously unknown duration and bandwidth. Computationally efficient modulators and demodulators are suggested for the scheme, and the results of a preliminary performance evaluation are presented. Although not yet a fully developed protocol, fractal modulation represents a potentially viable paradigm for communication.**

Index Terms—**Fractals, wavelets, modulation theory, spread spectrum.**

I. Introduction

SIGNALS with self-similar properties, i.e., signals which retain many of their essential characteristics under time scaling arise frequently in physical processes and also are potentially important in signal generation for communications, remote sensing, and many other applications. The most extensively studied class of such signals are those random processes which exhibit *statistical* self-similarity, e.g., processes whose autocorrelation functions remain invariant to within an amplitude factor under arbitrary scalings of the time axis. An important family of such random processes are typically referred to as $1/f$ processes. These processes are often used in modeling natural landscapes, the distribution of earthquakes, ocean waves, turbulent flow, the pattern of errors on communication channels, and many other natural phenomena.

In this paper, we consider signals that exhibit *deterministic* self-similarity, whereby the signal itself remains invariant to within an amplitude factor under arbitrary scaling of the time axis. This class of signals, referred to as homogeneous signals [1], is fairly restricted. However, by generalizing the class of homogeneous signals to require self-similarity only under time scaling by integer powers of two, a family of signals results with potential use as waveforms in a range of engineering applications. As an example of one promising direction for applications, we consider the use of generalized homogeneous signal sets in a communications-based context. Specifically, we develop an approach for embedding information into homogeneous waveforms that we term "fractal modulation." Because the resulting waveforms have the property that the information is contained within multiple time scales and frequency bands, we are able to show that such signals are well-suited for transmission over noisy channels of simultaneously unknown duration and bandwidth. This a reasonable model not only for many physical channels, but also for the receiver constraints inherent in many point-to-point and broadcast communication scenarios. While this proposed modulation scheme is very preliminary and there are many unresolved issues to be explored, it is suggestive of potential ways in which homogeneous signals can perhaps be exploited.

Our approach to the analysis and representation of these generalized homogeneous signals is based on the use of orthonormal wavelet bases. These bases, which have the property that all basis functions are dilations and translations of some prototype function, are in many respects ideally suited for use with self-similar signals [2]. Furthermore, because wavelet transformations can be implemented in a computationally efficient manner, the wavelet transform is not only a theoretically important tool, but a practical one as well.

In Section II, we briefly summarize the notation and properties of wavelet bases to be used in the remainder of the paper. Section III introduces and develops the generalized family of homogeneous signals defined in terms of a dyadic scale-invariance property. We distinguish between two classes: energy-dominated and power-dominated, and develop their spectral properties. We show that orthonormal self-similar bases can be constructed for these signals using wavelets. Using these representations, we then derive efficient discrete-time algorithms for synthesizing and analyzing such signals. Section IV develops the concept of fractal modulation. In particular, we use the orthonormal self-similar basis expansions derived in Section III to develop an

Manuscript received February 28, 1991; revised November 4, 1991.
The authors are will the Research Laboratory of Electronics, Massachusetts Institute of Technology, Room 36-615, Cambridge, MA 02139.
IEEE Log Number 9105482.

approach for modulating information sequences onto homogeneous signals. After developing the corresponding optimal receiver, we evaluate the performance of the resulting scheme in the context of a particular channel model and make comparisons to more traditional forms of modulation. Finally, Section V summarizes the principal contributions of the paper and suggests some interesting and potentially important directions for future research.

II. Wavelet Notation

In this section, we establish the notational conventions and terminology for the aspects of wavelet theory we shall exploit in this paper. For a more general review of the theory of orthonormal wavelet bases, see, e.g., the classic references [3], [4].

An orthonormal wavelet transformation of a signal $x(t)$ is described in terms of the synthesis/analysis equations[1]

$$x(t) = \sum_m \sum_n x_n^m \psi_n^m(t) \tag{1a}$$

$$x_n^m = \int_{-\infty}^{\infty} x(t)\psi_n^m(t)\,dt \tag{1b}$$

and has the special property that the orthogonal basis functions are all dilations and translations of a single function referred to as the *basic wavelet* $\psi(t)$. In particular,

$$\psi_n^m(t) = 2^{m/2}\psi(2^m t - n), \tag{2}$$

where m and n are the dilation and translation indices, respectively.

The Fourier transform of the basic wavelet, denoted $\Psi(\omega)$, often has a bandpass character, at least roughly. As a consequence, wavelet decompositions may be interpreted rather naturally in terms of a critically sampled generalized constant-Q or octave-band filter bank. In fact, an example of a wavelet basis, and one which will play an important role in this paper, is the ideal bandpass wavelet basis. In this specific case, the Fourier transform of the wavelet, which we denote by $\tilde{\Psi}(\omega)$, is

$$\tilde{\Psi}(\omega) = \begin{cases} 1, & \pi < |\omega| \le 2\pi, \\ 0, & \text{otherwise}. \end{cases} \tag{3}$$

In many applications, it is useful to impose some degree of regularity on the wavelet basis. As is well known [4], a sufficient condition for a wavelet basis to possess Rth-order regularity

$$\Psi(\omega) \sim O(|\omega|^{-R}), \qquad |\omega| \to \infty,$$

where R is some positive integer, is that the wavelet have R vanishing moments, i.e.,

$$\int_{-\infty}^{\infty} t^r \psi(t)\,dt = (j)^r \Psi^{(r)}(0) = 0, \quad r = 0, 1, \cdots, R-1.$$

Many examples of wavelets with such regularity have been developed in the literature; see, e.g., [4].

A broad class of orthonormal wavelet bases may also be conveniently interpreted in terms of multiresolution signal analysis. Associated with each such wavelet basis is a corresponding scaling function $\phi(t)$ having a Fourier transform $\Phi(\omega)$ that is at least roughly lowpass. The scaling function associated with the ideal bandpass wavelet basis, in fact, has an ideal lowpass Fourier transform

$$\tilde{\Phi}(\omega) = \begin{cases} 1, & |\omega| \le \pi, \\ 0, & \text{otherwise}. \end{cases}$$

A resolution-limited approximation $A_m x(t)$ to a signal $x(t)$ in which details on scales 2^m and finer are discarded is obtained via the orthonormal expansion

$$A_m x(t) = \sum_n a_n^m \phi_n^m(t), \tag{4}$$

where the $\phi_n^m(t)$ are also all dilations and translations of one another, viz.,

$$\phi_n^m(t) = 2^{m/2}\phi(2^m t - n),$$

and where the coefficients a_n^m are obtained by projection:

$$a_n^m = \int_{-\infty}^{\infty} x(t)\phi_n^m(t)\,dt. \tag{5}$$

For these signal approximations, the detail signal $D_m x(t)$ capturing the information in $x(t)$ between scales 2^m and 2^{m+1} has the orthonormal expansion

$$D_m x(t) = A_{m+1}x(t) - A_m x(t) = \sum_n x_n^m \psi_n^m(t).$$

The multiresolution signal analysis interpretation of wavelet bases also leads to efficient discrete-time algorithms for implementing wavelet transformations. In particular, associated with every wavelet-based multiresolution analysis is a quadrature mirror filter (QMF) pair whose unit-sample responses $h[n]$ and $g[n]$ have at least roughly low-pass and high-pass discrete-time Fourier transforms $H(\omega)$ and $G(\omega)$, respectively. These filters are exploited in the following filter-downsample analysis algorithm

$$a_n^m = \sum_l h[l - 2n]\, a_l^{m+1}, \tag{6a}$$

$$x_n^m = \sum_l g[l - 2n]\, a_l^{m+1}, \tag{6b}$$

which may be applied recursively to extract the wavelet coefficients x_n^m at successively coarser scales. In a complementary manner, the following upsample-filter-merge synthesis algorithm

$$a_n^{m+1} = \sum_l \{h[n - 2l]\, a_l^m + g[n - 2l]\, x_l^m\} \tag{6c}$$

may be applied recursively to reconstruct the coefficients a_n^m of an increasingly fine-scale approximation to a signal $x(t)$. Collectively, (6) constitute what has become known as the discrete wavelet transform (DWT).

III. Deterministically Self-Similar Signals

Signals $x(t)$ satisfying the deterministic scale-invariance property

$$x(t) = a^{-H}x(at), \tag{7}$$

[1] We shall assume throughout that all summations over m and n extend from $-\infty$ to ∞ unless otherwise noted.

for all $a > 0$, are generally referred to in mathematics as *homogeneous* functions of degree H. As shown by Gel'fand [1], homogeneous functions can be parameterized with only a few constants. As such, they constitute a rather limited class of signal models in many contexts.

A comparatively richer class of signal models is obtained by considering waveforms which are required to satisfy (7) only for values of a that are integer powers of two, i.e., signals that satisfy the dyadic self-similarity property

$$x(t) = 2^{-kH}x(2^k t), \tag{8}$$

for all integers k. While we shall use the generic term "homogeneous signal" to refer to signals satisfying (8), when there is risk of confusion in our subsequent development we will specifically refer to signals satisfying (8) as *dy-homogeneous.*

Homogeneous signals have spectral characteristics very much like those of $1/f$ processes and, in fact, have fractal properties as well. Specifically, although all nontrivial homogeneous signals have infinite energy and many have infinite power, there are nevertheless some such signals with which one can associate a generalized $1/f$-like Fourier transform, and others with which one can associate a generalized $1/f$-like power spectrum. We distinguish between these two classes of homogeneous signals in our subsequent treatment, denoting them *energy-dominated* and *power-dominated* homogeneous signals, respectively. As we develop in Sections III-A and III-B, orthonormal wavelet basis expansions constitute particularly convenient and efficient representations for these two classes of signals.

A. Energy-Dominated Homogeneous Signals

Definition 1: A dy-homogeneous signal $x(t)$ is said to be energy-dominated if when $x(t)$ is filtered by an ideal bandpass filter with frequency response

$$B_0(\omega) = \begin{cases} 1, & \pi < |\omega| \le 2\pi, \\ 0, & \text{otherwise}, \end{cases} \tag{9}$$

the resulting signal $\tilde{x}_0(t)$ has finite-energy, i.e.,

$$\int_{-\infty}^{\infty} \tilde{x}_0^2(t)\, dt < \infty.$$

The choice of passband edges at π and 2π in our definition is, in fact, somewhat arbitrary. In particular, substituting in the definition any passband that includes one entire frequency octave but does not include $\omega = 0$ or $\omega = \infty$ leads to precisely the same class of signals. However, our particular choice is sufficient and is made in anticipation of the representation of this class of signals in terms of a wavelet basis.

The class of energy-dominated homogeneous signals includes both reasonably regular functions, such as the constant $x(t) = 1$, the ramp $x(t) = t$, the time-warped sinusoid $x(t) = \cos[2\pi \log_2 t]$, and the unit step function $x(t) = u(t)$, as well as singular functions, such as $x(t) = \delta(t)$ and its derivatives. We denote by $\boldsymbol{E}^H$ the collection of all energy-dominated homogeneous signals of degree H. The following theorem allows us to interpret the notion of spectra for such signals. A straightforward but detailed proof is provided in Appendix A.

Theorem 1: When an energy-dominated homogeneous signal $x(t)$ of degree H is filtered by an ideal bandpass filter with frequency response

$$B(\omega) = \begin{cases} 1, & \omega_L < |\omega| \le \omega_U, \\ 0, & \text{otherwise}, \end{cases} \tag{10}$$

for arbitrary $0 < \omega_L < \omega_U < \infty$, the resulting signal $y(t)$ has finite energy and a Fourier transform of the form

$$Y(\omega) = \begin{cases} X(\omega), & \omega_L < |\omega| \le \omega_U, \\ 0, & \text{otherwise}, \end{cases} \tag{11}$$

where $X(\omega)$ is some function that is independent of ω_L and ω_U and has octave-spaced ripple, i.e., for all integers k,

$$|\omega|^{H+1} X(\omega) = |2^k \omega|^{H+1} X(2^k \omega). \tag{12}$$

Since in this theorem $X(\omega)$ does not depend on ω_L or ω_U, this function may be interpreted as the generalized Fourier transform of $x(t)$. Furthermore, (12) implies that the generalized Fourier transform of signals in $\boldsymbol{E}^H$ obeys a $1/f$-like (power-law) relationship, viz.,

$$|X(\omega)| \sim \frac{1}{|\omega|^{H+1}}.$$

We note that because (11) excludes $\omega = 0$ and $\omega = \infty$, the mapping

$$x(t) \leftrightarrow X(\omega)$$

is not one to one. As an example, $x(t) = 1$ and $x(t) = 2$ are both in $\boldsymbol{E}^H$ for $H = 0$, yet both have $X(\omega) = 0$ for $\omega > 0$. In order to accommodate this behavior in our subsequent theoretical development, all signals having a common $X(\omega)$ will be combined into an equivalence class. For example, two homogeneous functions $f(t)$ and $g(t)$ are equivalent if they differ by a homogeneous function whose frequency content is concentrated at the origin, such as t^H in the case that H is an integer.

Because the dyadic self-similarity property (8) of dy-homogeneous signals is very similar to the dyadic scaling relationship between basis functions in an orthonormal wavelet basis, wavelets provide a particularly nice representation for this family of signals. Specifically, with $x(t)$ denoting an energy-dominated homogeneous signal, the expansion in an orthonormal wavelet basis is

$$x(t) = \sum_m \sum_n x_n^m \psi_n^m(t) \tag{13a}$$

$$x_n^m = \int_{-\infty}^{\infty} x(t)\psi_n^m(t). \tag{13b}$$

Since $x(t)$ satisfies (8) and since $\psi_n^m(t)$ satisfies (2), it easily follows from (13b) that for homogeneous signals

$$x_n^m = \beta^{-m/2} x_n^0, \tag{14}$$

where

$$\beta = 2^{2H+1} = 2^{\gamma}. \tag{15}$$

Denoting x_n^0 by $q[n]$, (13a) then becomes

$$x(t) = \sum_m \sum_n \beta^{-m/2} q[n] \psi_n^m(t), \tag{16}$$

from which we see that $x(t)$ is completely specified in terms of $q[n]$. We term $q[n]$ a *generating sequence* for $x(t)$ since, as we shall see, this representation leads to techniques for synthesizing useful approximations to homogeneous signals in practice.

Let us now specifically choose the ideal bandpass wavelet basis, whose basis functions we denote by

$$\tilde{\psi}_n^m(t) = 2^{m/2} \tilde{\psi}(2^m t - n),$$

where $\tilde{\psi}(t)$ is the ideal bandpass wavelet whose Fourier transform is given by (3). If we sample the output $\tilde{x}_0(t)$ of the filter in Definition 1 at unit rate, we obtain the sequence $\tilde{q}[n] = \tilde{x}_n^0$, where $\tilde{x}_n^m$ denotes the coefficients of expansion of $x(t)$ in terms of the ideal bandpass wavelet basis. Since $\tilde{x}_0(t)$ in Definition 1 has the orthonormal expansion

$$\tilde{x}_0(t) = \sum_n \tilde{q}[n] \tilde{\psi}_n^0(t) \tag{17}$$

we have

$$\int_{-\infty}^{\infty} \tilde{x}_0^2(t)\, dt = \sum_n \tilde{q}^2[n]. \tag{18}$$

Consequently, a homogeneous function is energy-dominated, if and only if its generating sequence in terms of the ideal bandpass wavelet basis has finite energy, i.e.,

$$\sum_n \tilde{q}^2[n] < \infty.$$

A convenient inner product between two energy-dominated homogeneous signals $f(t)$ and $g(t)$ can be defined as

$$\langle f, g \rangle_{\tilde{\psi}} = \int_{-\infty}^{\infty} f_0(t) g_0(t)\, dt$$

where the signals $f_0(t)$ and $g_0(t)$ are the responses of the bandpass filter (9) to $f(t)$ and $g(t)$, respectively. Exploiting (17) we may more conveniently express this inner product in terms of $\tilde{a}[n]$ and $\tilde{b}[n]$, the respective generating sequences of $f(t)$ and $g(t)$ under the bandpass wavelet basis, as

$$\langle f, g \rangle_{\tilde{\psi}} = \sum_n \tilde{a}[n] \tilde{b}[n]. \tag{19}$$

With this inner product, $\boldsymbol{E}^H$ constitutes a Hilbert space and the induced norm on $\boldsymbol{E}^H$ is

$$\| x \|_{\tilde{\psi}} = \int_{-\infty}^{\infty} \tilde{x}_0^2(t)\, dt = \sum_n \tilde{q}^2[n]. \tag{20}$$

One can readily construct "self-similar" bases for $\boldsymbol{E}^H$. Indeed, the ideal bandpass wavelet (16) immediately provides an orthonormal basis for $\boldsymbol{E}^H$. In particular, for any $x(t) \in \boldsymbol{E}^H$, we have the synthesis/analysis pair

$$x(t) = \sum_n \tilde{q}[n] \tilde{\theta}_n^H(t) \tag{21a}$$

$$\tilde{q}[n] = \langle x, \tilde{\theta}_n^H \rangle_{\tilde{\psi}} \tag{21b}$$

where one can easily verify that the basis functions

$$\tilde{\theta}_n^H(t) = \sum_m \beta^{-m/2} \tilde{\psi}_n^m(t) \tag{22}$$

are self-similar, orthogonal, and have unit norm.

The fact that the ideal bandpass basis is unrealizable means that (21) is not a practical mechanism for synthesizing or analyzing homogeneous signals. However, more practical wavelet bases are equally suitable for defining an inner product for the Hilbert space $\boldsymbol{E}^H$. In fact, we shall show that a broad class of wavelet bases can be used to construct such inner products, and that, as a consequence, some highly efficient algorithms arise for processing homogeneous signals.

Not every orthonormal wavelet basis can be used to define inner products for $\boldsymbol{E}^H$. In order to determine which orthonormal wavelet bases can be used to define inner products for $\boldsymbol{E}^H$, we must determine for which wavelets $\psi(t)$

$$q[n] = \int_{-\infty}^{\infty} x(t) \psi_n^0(t)\, dt \in l^2(\boldsymbol{Z}) \Leftrightarrow$$

$$x(t) = \sum_m \sum_n \beta^{-m/2} q[n] \psi_n^m(t) \in \boldsymbol{E}^H.$$

That is, we seek conditions on a wavelet basis such that the sequence

$$q[n] = \int_{-\infty}^{\infty} x(t) \psi_n^0(t)\, dt$$

has finite energy whenever the homogeneous signal $x(t)$ is energy-dominated, and simultaneously such that the homogeneous signal

$$x(t) = \sum_m \sum_n \beta^{-m/2} q[n] \psi_n^m(t)$$

is energy-dominated whenever the sequence $q[n]$ has finite energy. Our main result is presented in terms of the following theorem. A proof of this theorem is provided in Appendix B.

Theorem 2: Consider an orthonormal wavelet basis such that $\psi(t)$ has R vanishing moments for some integer $R \geq 1$, i.e.,

$$\Psi^{(r)}(0) = 0, \qquad r = 0, 1, \cdots, R-1 \tag{23}$$

and let

$$x(t) = \sum_m \sum_n \beta^{-m/2} q[n] \psi_n^m(t)$$

be a dy-homogeneous signal whose degree H is such that $\gamma = \log_2 \beta = 2H + 1$ satisfies $0 < \gamma < 2R - 1$. Then $x(t)$ is energy-dominated, if and only if $q[n]$ has finite energy.

This theorem implies that we may choose for our Hilbert space $\boldsymbol{E}^H$ from among a large number of inner products

whose induced norms are all equivalent. In particular, for any wavelet $\psi(t)$ with sufficiently many vanishing moments, we may define the inner product between two functions $f(t)$ and $g(t)$ in $\boldsymbol{E}^H$ whose generating sequences are $a[n]$ and $b[n]$, respectively, as

$$\langle f, g\rangle_\psi = \sum_n a[n]\, b[n]. \tag{24}$$

Of course, this collection of inner products is almost surely not exhaustive. Even for wavelet-based inner products, Theorem 2 asserts only that the vanishing moment condition is sufficient to ensure that the inner product generates an equivalent norm. It seems unlikely that the vanishing moment condition is a necessary condition.

The wavelet-based norms for $\boldsymbol{E}^H$ constitute a highly convenient and practical collection from which to choose in applications involving the use of homogeneous signals. Indeed, each associated wavelet-based inner product leads immediately to an orthonormal self-similar basis for $\boldsymbol{E}^H$: if $x(t) \in \boldsymbol{E}^H$, then

$$x(t) = \sum_n q[n]\theta_n^H(t) \tag{25a}$$

$$q[n] = \langle x, \theta_n^H\rangle_\psi, \tag{25b}$$

where, again, the basis functions

$$\theta_n^H(t) = \sum_m \beta^{-m/2}\, \psi_n^m(t) \tag{26}$$

are all self-similar, mutually orthogonal, and have unit norm.

Finally, we remark that wavelet-based characterizations also give rise to a convenient expression for the generalized Fourier transform of an energy-dominated homogeneous signal $x(t)$. In particular, if we take the Fourier transform of (16) we get, via some routine algebra,

$$X(\omega) = \sum_m 2^{-(H+1)m}\Psi(2^{-m}\omega)Q(2^{-m}\omega), \tag{27}$$

where $Q(\omega)$ is the discrete-time Fourier transform of $q[n]$. This spectrum is to be interpreted in the sense of Theorem 1, i.e., $X(\omega)$ defines the spectral content of the output of a bandpass filter at every frequency ω within the passband.

B. Power-Dominated Homogeneous Signals

Energy-dominated homogeneous signals have infinite energy. In fact, most have infinite power as well. However, there are other infinite power homogeneous signals that are not energy-dominated. In this section, we consider a more general class of infinite-power homogeneous signals referred to as power-dominated homogeneous signals which will find application in Section IV. The definition and properties closely parallel those for energy-dominated homogeneous signals.

Definition 2: A dy-homogeneous signal $x(t)$ is said to be power-dominated if when $x(t)$ is filtered by an ideal bandpass filter with frequency response (9) the resulting signal $\tilde{x}_0(t)$ has finite power, i.e.,

$$\lim_{T\to\infty} \frac{1}{2T}\int_{-T}^{T} \tilde{x}_0^2(t)\, dt < \infty.$$

The notation $\boldsymbol{P}^H$ will be used to designate the class of power-diminated homogeneous signals of degree H. Moreover, while our definition necessarily includes the energy dominated signals, which have zero power, insofar as our discussion is concerned they constitute a degenerate case.

Analogous to Theorem 1 for the energy-dominated case, we can establish the following theorem describing the spectral properties of power-dominated homogeneous signals.

Theorem 3: When a power-dominated homogeneous signal $x(t)$ is filtered by an ideal band-pass filter with frequency response (10), the resulting signal $y(t)$ has finite power and a power spectrum of the form

$$S_y(\omega) = \lim_{T\to\infty} \frac{1}{2T}\left|\int_{-T}^{T} y(t)e^{-j\omega t}\, dt\right|^2 = \begin{cases} S_x(\omega), & \omega_L < |\omega| \le \omega_U, \\ 0, & \text{otherwise}, \end{cases} \tag{28}$$

where $S_x(\omega)$ is some function that is independent of ω_L and ω_U and has octave-spaced ripple, i.e., for all integers k,

$$|\omega|^{2H+1} S_x(\omega) = |2^k\omega|^{2H+1} S_x(2^k\omega). \tag{29}$$

The details of the proof of this theorem are contained in Appendix C, although it is identical in style to the proof of its counterpart, Theorem 1. Note that since $S_x(\omega)$ in the theorem does not depend on ω_L or ω_U, this function may be interpreted as the generalized power spectrum of $x(t)$. Furthermore, the relation (29) implies that signals in $\boldsymbol{P}^H$ have a generalized time-averaged power spectrum that is $1/f$-like, i.e.,

$$S_x(\omega) \sim \frac{1}{|\omega|^\gamma}, \tag{30}$$

where, via (15), $\gamma = 2H + 1$.

Theorem 3 directly implies that a homgeneous signal $x(t)$ is power-dominated, if and only if its generating sequence $\tilde{q}[n]$ in the ideal bandpass wavelet basis has finite power, i.e.,

$$\sum_{L\to\infty} \frac{1}{2L+1} \sum_{n=-L}^{L} \tilde{q}^2[n] < \infty.$$

Similarly we can readily deduce from the results of Section III-A that, in fact, for any orthonormal wavelet basis with sufficiently many vanishing moments R so that $0 < \gamma < 2R - 1$, the *generating sequence* for a homogeneous signal of degree H in that basis has finite power, if and only if the signal is power-dominated. This implies that when we use (25a) with such wavelets to synthesize a homogeneous signal $x(t)$ using an arbitrary finite power sequence $q[n]$, we are assured that $x(t) \in \boldsymbol{P}^h$. Likewise, when we use (25b) to analyze any signal $x(t) \in \boldsymbol{P}^H$, we are assured that $q[n]$ has finite power.

Remarks: Energy-dominated homogeneous signals of arbitrary degree H can be highly regular, at least away from $t = 0$. In contrast, power-dominated homogeneous signals typically have a fractal structure similar to the statistically

self-similar $1/f$ processes of corresponding degree H, whose power spectra are also of the form (30) with $\gamma = 2H + 1$. One might reasonably conjecture that power-dominated homogeneous signals and $1/f$ processes of the same degree also have identical Hausdorff–Besicovitch dimensions [5], when defined. Indeed, despite their obvious structural differences, power-dominated homgeneous signals and $1/f$ processes "look" remarkably similar in a qualitative sense. This is apparent in Fig. 1, where we depict the sample path of a $1/f$ process along side a power-dominated homgeneous signal of the same degree whose generating sequence has been taken from a white random process. We stress that in Fig. 1(a), the self-similarity of the $1/f$ process is statistical, i.e., it does not satisfy (8) but its autocorrelation function does. In Fig. 1(b), the self-similarity of the homogeneous signal is deterministic. In fact, while the wavelet coefficients of homogeneous signals are identical from scale to scale to within an amplitude factor, i.e.,

$$x_n^m = \beta^{-m/2} q[n],$$

the wavelet coefficients of $1/f$ processes have only the same second-order statistics from scale to scale to within an amplitude factor, i.e.,

$$E[x_n^m x_l^m] = \beta^{-m} \rho[n - l],$$

for some function $\rho[n]$ that is independent of m [2], [6].

Finally, we remark that not all power-dominated homogeneous signals have spectra that are bounded on $\pi \leq \omega \leq 2\pi$. An interesting subclass of power-dominated homogeneous signals with such unbounded spectra will, in fact, arise in our development of fractal modulation. For these signals, $\tilde{x}_0(t)$ as defined in Definition 2 is *periodic*, so we refer to this class of power-dominated homogeneous signals as *periodicity-dominated*. It is straightforward to establish that these homogeneous signals have the property that when passed through an arbitrary bandpass filter of the form (10) the output is periodic as well. Furthermore, their power spectra consist of impulses whose *areas* decay according to a $1/|\omega|^{\gamma}$ relationship. An important class of periodicity-dominated homogeneous signals can be generated through a wavelet-based synthesis of the form (16) in which the generating sequence $q[n]$ is periodic.

C. Discrete-Time Algorithms for Processing Homogeneous Signals

Orthonormal wavelet representations provide some useful insights into homogeneous signals. For instance, because the sequence $q[n]$ is replicated at each scale in the representation (16) of homogeneous signal $x(t)$, the detail signals

$$D_m x(t) = \beta^{-m/2} \sum_n q[n] \psi_n^m(t),$$

representing $q[n]$ modulated into a particular octave band are simply time-dilated versions of one another, to within an amplitude factor. The corresponding time-frequency portrait of a homogeneous signal is depicted in Fig. 2, from which the scaling properties are apparent. For purposes of illustration, the signal in this figure has degree $H = -1/2$ (i.e., $\beta = 1$), which corresponds to the case in which $q[n]$ is scaled by the same amplitude factor in each octave band. Clearly, the partitioning in such time-frequency portraits is idealized: in general, there is both spectral and temporal overlap between cells.

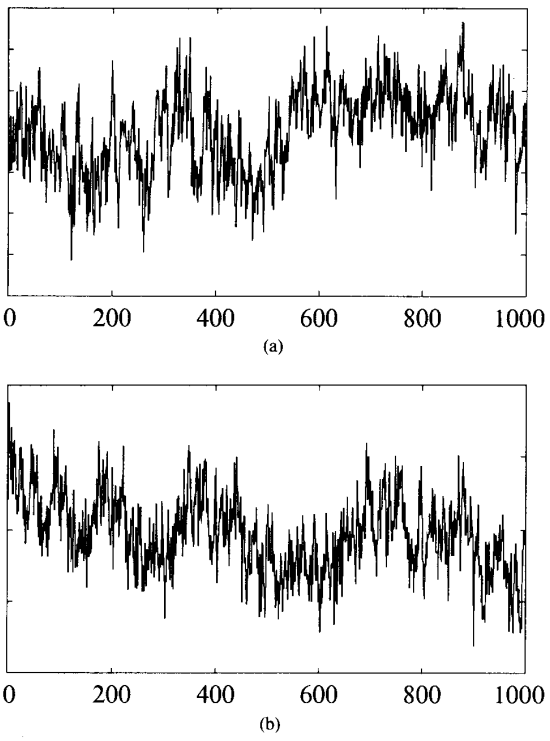

Fig. 1. Comparison between the sample path of a $1/f$ process (a) and a power-dominated homogeneous signal (b). Both correspond to $\gamma = 1$ (i.e., $H = 0$).

Wavelet representations also lead to some highly efficient algorithms for synthesizing, analyzing, and processing homogeneous signals just as they do for $1/f$ processes as discussed in [7]. The signal processing structures we develop in this section are a consequence of applying the DWT algorithm to the highly structured form of the wavelet coefficients of homogeneous signals.

We have already encountered one discrete-time representation for a homogeneous signal $x(t)$, namely that in terms of a generating sequence $q[n]$ that corresponds to the coefficients of the expansion of $x(t)$ in an orthonormal basis $\{\theta_n^H(t)\}$ for E^H. When the $\theta_n^H(t)$ are derived from a wavelet basis according to (26), another useful discrete-time representation for $x(t)$ is available, which we now discuss.

Consider the coefficients a_n^m characterizing the resolution-limited approximation $A_m x(t)$ of a homogeneous signal $x(t)$ with respect to a particular wavelet-based multiresolution signal analysis. Since these coefficients are the projections of $x(t)$ onto dilations and translations of the scaling function $\phi(t)$ according to (5), it is straightforward to verify that they, too, are identical at all scales to within an ampli-

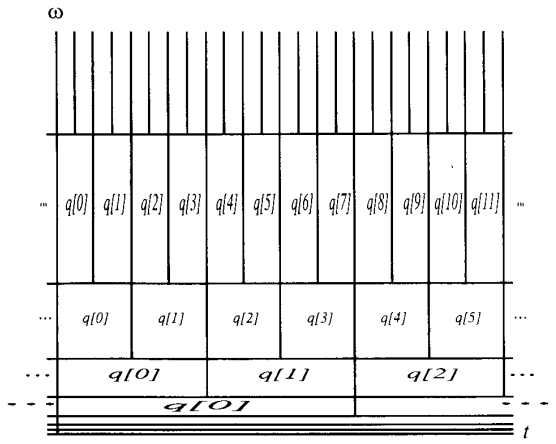

Fig. 2. Time-frequency portrait of a homogeneous signal ($H = -1/2$).

tude factor, i.e.,

$$a_n^m = \beta^{-m/2} a_n^0. \tag{31}$$

Consequently, the sequence a_n^0 is an alternative discrete-time characterization of $x(t)$, since knowledge of it is sufficient to reconstruct $x(t)$ to arbitrary accuracy. For convenience, we refer to a_n^0 as the *characteristic sequence* and denote it as $p[n]$. As is true for the generating sequence, the characteristic sequence associated with $x(t)$ depends upon the particular multiresolution analysis used; distinct multiresolution signal analyses generally yield different characteristic sequences for any given homogeneous signal. We shall require that the wavelet associated with any multiresolution analysis we consider have sufficiently many vanishing moments that it meets the conditions of Theorem 2.

The characteristic sequence $p[n]$ is associated with a resolution-limited approximation to the corresponding homogeneous signal $x(t)$. Specifically, $p[n]$ represents unit-rate samples of the output of the filter, driven by $x(t)$, whose frequency response is the complex conjugate of $\Phi(\omega)$. Because frequencies in the neighborhood of the spectral origin, where the spectrum of $x(t)$ diverges, are passed by such a filter, $p[n]$ will often have infinite energy or, worse, infinite power, even when the generating sequence $q[n]$ has finite energy.

The characteristic sequence can, in fact, be viewed as a *discrete-time* homogeneous signal, and a theory can be developed following an approach directly analogous to that used in Sections III-A and III-B for the case of continuous-time homogeneous signals. The characteristic sequence satisfies the discrete-time self-similarity relation[2]

$$\beta^{1/2} p[n] = \sum_k h[k - 2n]\, p[k], \tag{32}$$

which is readily obtained by substituting for a_n^m in the DWT analysis equation (6a) using (31) and that $a_n^0 = p[n]$. Indeed, as depicted in Fig. 3, (32) is a statement that when $p[n]$ is low-pass filtered with the conjugate filter whose unit-sample response is $h[-n]$ and then downsampled, we recover an amplitude-scaled version of $p[n]$. Although characteristic sequences are, in an appropriate sense, "generalized sequences," when high-pass filtered with the corresponding conjugate highpass filter whose unit-sample response is $g[-n]$, the output is a finite energy or finite power sequence, depending on whether $p[n]$ corresponds to a homogeneous signal $x(t)$ that is energy-dominated or power-dominated, respectively. Consequently, we can analogously classify the sequence $p[n]$ as energy-dominated in the former case, and power-dominated in the latter case. In fact, when the output of such a high-pass filter is downsampled at rate two, we recover the characteristic sequence $q[n]$ associated with the expansion of $x(t)$ in the corresponding wavelet basis, i.e.,

$$\beta^{1/2} q[n] = \sum_k g[k - 2n]\, p[k]. \tag{33}$$

This can be readily verified by substituting for a_n^m and x_n^m in the DWT analysis equation (6b) using (31) and (14), and by recognizing that $a_n^0 = p[n]$ and $x_n^0 = q[n]$.

From a different perspective, (33) provides a convenient mechanism for obtaining the representation for a homogeneous signal $x(t)$ in terms of its generating sequence $q[n]$ from one in terms of its corresponding characteristic sequence $p[n]$, i.e.,

$$p[n] \rightarrow q[n].$$

To obtain the reverse mapping

$$q[n] \rightarrow p[n]$$

is less straightforward. For an arbitrary sequence $q[n]$, the associated characteristic sequence $p[n]$ is the solution to the linear equation

$$\beta^{-1/2} p[n] - \sum_k h[n - 2k]\, p[k] = \sum_k g[n - 2k]\, q[k], \tag{34}$$

as as can be verified by specializing the DWT synthesis equation (6c) to the case of homogeneous signals. There appears to be no direct method for solving this equation. However, the DWT synthesis algorithm suggests a convenient and efficient iterative algorithm for constructing $p[n]$ from $q[n]$. In particular, denoting the estimate of $p[n]$ on the ith iteration by $p^{[i]}[n]$, the algorithm is

$$p^{[0]}[n] = 0 \tag{35a}$$

$$p^{[i+1]}[n] = \beta^{1/2} \sum_k \{h[n - 2k]\, p^{[i]}[k] + g[n - 2k]\, q[k]\}. \tag{35b}$$

This recursive upsample-filter-merge algorithm, depicted in Fig. 4, can be interpreted as repeatedly modulating $q[n]$ with the appropriate gain into successively lower octave bands of the frequency interval $0 \leq |\omega| \leq \pi$. Note that the

[2] Relations of this type may be considered discrete-time counterparts of the *dilation equations* considered by Strang in [8].

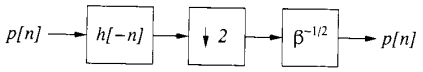

Fig. 3. Discrete-time self-similarity identity for a characteristic sequence $p[n]$.

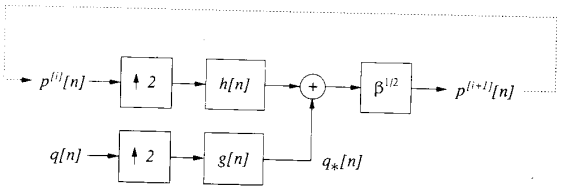

Fig. 4. Interative algorithm for the synthesis of the characteristic sequence $p[n]$ of a homogeneous signal $x(t)$ from its generating sequence $q[n]$. Notation $p^{[i]}[n]$ denotes the value of $p[n]$ at the ith iteration.

precomputable quantity

$$q_*[n] = \sum_k g[n - 2k]q[k]$$

represents the sequence $q[n]$ modulated into essentially the upper half band of frequencies.

Any real application of homogeneous signals can ultimately exploit scaling properties over only a *finite* range of scales, so that it suffices in practice to modulate $q[n]$ into a finite range of contiguous octave bands. Consequently, only a finite number of iterations of the algorithm (35) are ever required. More generally, this also means that many of the theoretical issues associated with homogeneous signals concerning singularities and convergence do not present practical difficulties in the application of these signals, as will be apparent in our developments of Section IV.

Before turning to a potential application of homogeneous signal sets, we mention that there would appear to be important connections to be explored between the theory of self-similar signals described here and the work of Barnsley, *et al.*, [9] on deterministically self-affine signals. Interestingly, the recent work of Malassenet and Mersereau [10] has shown that these signals, which are conveniently generated using so-called "iterated function systems" have efficient representations in terms of wavelet bases as well.

IV. Fractal Modulation

In this section, we consider the use of homogeneous signals as modulating waveforms in a communications-based context as an example of the direction that some applications may take. Beginning with an idealized but fairly general channel model, we demonstrate that the use of homogeneous waveforms in such channels is at least natural, if not optimal, and leads to a multirate modulation strategy in which data is transmitted simultaneously at multiple rates. While it is a preliminary proposal, the modulation has a number of properties that seem appealing.

Our problem involves the design of a communication system for transmitting a continuous- or discrete-valued data sequence over a noisy and unreliable continuous-amplitude, continuous-time channel. We must, therefore, design a modulator at the transmitter than embeds the data sequence $q[n]$ into a signal $x(t)$ to be sent over the channel. At the receiver, a demodulator must be designed for processing the distorted signal $r(t)$ from the channel to extract an optimal estimate of the data sequence $\hat{q}[n]$.

In a typical communication scenario, the channel would be "open" for some time interval T, during which it has a particular bandwidth W and signal-to-noise ratio (SNR). Such a channel model can be used to capture both characteristics of the transmission medium and constraints inherent in one or more receivers. When the noise characteristics are additive, the overall channel model is as depicted in Fig. 5, where $z(t)$ represents the noise process.

When either the bandwidth or duration parameters of the channel are known *a priori*, there are many well-established methodologies for designing an efficient and reliable communication system. However, we shall restrict our attention to the case in which *both* the bandwidth and duration parameters are either unknown or not available to the transmitter. This case, by contrast, has received comparatively less attention in the communications literature, although it encompasses a range of both point-to-point and broadcast communication scenarios involving, for example, jammed and fading channels, multiple access channels, covert and low probability of intercept (LPI) communication, and broadcast communication to disparate receivers.

We shall require the communication system we design for such channels to satisfy the following performance characteristics.

1) Given a duration-bandwidth product $T \times W$ that exceeds some threshold, we must be able to transmit $q[n]$ without error in thee absence of noise, i.e., $z(t) = 0$.
2) Given increasing duration-bandwidth product in excess of this threshold, we must be able to transmit $q[n]$ with increasing fidelity in the presence of noise. Furthermore, in the limit of infinite duration-bandwidth product, perfect transmission should be achievable at any finite SNR.

The first of these requirements implies that, at least in principle, we ought to be able to recover $q[n]$ using arbitrarily narrow receiver bandwidth given sufficient duration, or alternatively, from an arbitrarily short duration segment given sufficient bandwidth. The second requirement implies that we ought to be able to obtain better estimates of $q[n]$ the longer a receiver is able to listen, or the greater the bandwidth it has available. Consequently, the modulation must contain redundancy of a type that can be exploited for the purposes of error correction. As we shall demonstrate, the use of homogeneous signals for transmission appears to be rather naturally suited to fulfilling both these system requirements.

The minimum achievable duration-bandwidth threshold in such a system is a measure of the efficiency of the modulation. Actually, because the duration-bandwidth threshold $T \times W$ is a function of the length L of the data sequence, it is more convenient to transform the duration constraint T into a symbol rate constraint $R = L/T$ and phrase the discussion

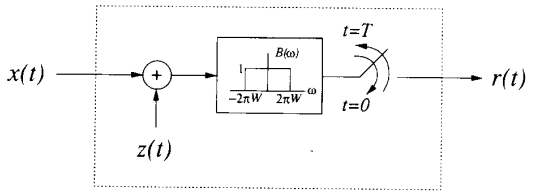

Fig. 5. Channel model for a typical communications scenario.

in terms of a rate-bandwidth threshold R/W that is independent of sequence length. Then, the maximum achievable rate-bandwidth threshold constitutes the *spectral efficiency* of the modulation, which we shall denote by η. The spectral efficiency of a transmission scheme using bandwidth W is, in fact, defined as

$$\eta = R_{\max}/W,$$

where $R_{\max}$ is the maximum rate at which perfect communication is possible in the absence of noise. Hence, the higher the spectral efficiency of a scheme, the higher the rate that can be achieved for a given bandwidth, or, equivalently, the smaller the bandwidth that is required to support a given rate.

When the available channel bandwidth is known *a priori*, a reasonably spectrally efficient, if impractical, modulation of a data sequence $q[n]$ involves expanding the sequence in terms of an ideally bandlimited orthonormal basis. Specifically, with W_0 denoting the channel bandwidth, a transmitter produces

$$x(t) = \sum_n q[n]\sqrt{W_0}\,\operatorname{sinc}(W_0 t - n),$$

where

$$\operatorname{sinc}(t) = \begin{cases} 1, & t = 0, \\ \dfrac{\sin \pi t}{\pi t}, & \text{otherwise.} \end{cases}$$

In the absence of noise, a receiver may recover $q[n]$ from the projections

$$q[n] = \int_{-\infty}^{\infty} x(t)\sqrt{W_0}\,\operatorname{sinc}(W_0 t - n)\,dt,$$

which can be implemented as a sequence of filter-and-sample operations. Since this scheme achieves a rate of $R = W_0$ symbols/sec using the double-sided bandwidth of $W = W_0$ Hz, it is characterized by a spectral efficiency of

$$\eta_0 = 1 \text{ symbol/s/Hz}. \tag{36}$$

However, because the transmitter is assumed to have perfect knowledge of the rate-bandwidth characteristics of the channel, this modulation does not constitute a viable solution to our communications problem. Indeed, in order to accommodate a decrease in available channel bandwidth, the transmitter would have to be accordingly reconfigured by decreasing the parameter W_0. Similarly, for the system to maintain a spectral efficiency of $\eta_0 = 1$ when the available channel bandwidth increases, the transmitter must be reconfigured by correspondingly increasing the parameter W_0. Nevertheless, while not a solution to our communications problem, this benchmark modulation provides a useful performance baseline in evaluating the fractal modulation strategy we develop.

We now turn our attention to the problem of designing a modulation strategy that maintains its spectral efficiency over a broad range of rate-bandwidth combinations using a fixed transmitter configuration. A rather natural solution to this problem arises out of the concept of embedding the data to be transmitted into a homogeneous signal. Due to the fractal properties of the transmitted signals, we refer to the resulting scheme as "fractal modulation."

A. Transmitter Design: Modulation

To embed a finite-power sequence $q[n]$ into a dy-homogeneous waveform $x(t)$ of degree H, it suffices to consider using $q[n]$ as the coefficients of an expansion in terms of a wavelet-based orthonormal self-similar basis of degree H, i.e.,

$$x(t) = \sum_n q[n]\theta_n^H(t),$$

where the basis functions $\theta_n^H(t)$ are constructed according to (26). When the basis is derived from the ideal bandpass wavelet, as we shall generally assume in our analysis, the resulting waveform $x(t)$ is a power-dominated homogeneous signal whose idealized time-frequency portrait has the form depicted in Fig. 2. Consequently, we may view this as a *multirate modulation* of $q[n]$ where in the mth frequency band $q[n]$ is modulated at rate 2^m using a double-sided bandwidth of 2^m Hz. Furthermore, the energy per symbol used in successively higher bands scales by $\beta^{-1} = 2^{-2H-1}$. Using a suitably designed receiver, $q[n]$ can, in principle, be recovered from $x(t)$ at an arbitrary rate 2^m using a baseband bandwidth of 2^{m+1} Hz. Consequently, this modulation has a spectral efficiency of

$$\eta_F = (1/2) \text{ symbol/s/Hz}.$$

We emphasize that in accordance with our channel model of Fig. 5, it is the baseband bandwidth that is important in defining the spectral efficiency since it identifies the highest frequency available at the receiver.

While the spectral efficiency of this modulation is half that of the benchmark scheme (36), this loss in efficiency is, in effect, the price paid to enable a receiver to use any of a range of rate-bandwidth combinations in demodulating the data. Fig. 6 illustrates the rate-bandwidth trade-offs available to the receiver. In the absence of noise the receiver can, in principle, perfectly recover $q[n]$ using rate-bandwidth combinations lying on or below the solid curve. The stepped character of this curve reflects the fact that only rates of the form 2^m can be accommodated, and that full octave increases in bandwidth are required to enable $q[n]$ to be demodulated at successively higher rates. For reference, the performance of our benchmark modulation is superimposed on this plot using a dashed line. We emphasize that in contrast to fractal modulation, the transmitter in the benchmark scheme re-

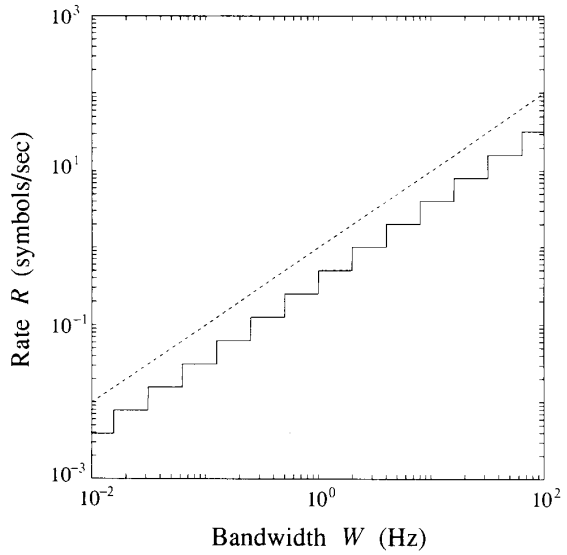

Fig. 6. Spectral efficiency of fractal modulation. At each bandwidth B, the solid curve indicates the maximum rate at which transmitted data can be perfectly recovered in the absence of noise. Dashed curve indicates the corresponding performance of the benchmark scheme.

quires perfect knowledge of the rate-bandwidth characteristics of the channel.

Although it considerably simplifies our analysis, the use of the ideal bandpass wavelet to synthesize the orthonormal self-similar basis in our modulation strategy is impractical due to the poor temporal localization in this wavelet. However, we may, in practice, replace the ideal bandpass wavelet with one having not only comparable frequency domain characteristics and better temporal localization, but sufficiently many vanishing moments to ensure that the transmitted waveform is power-dominated as well. Fortunately, there are many suitable wavelets from which to choose, among which are those due to Daubechies [4]. When such wavelets are used, the exact spectral efficiency of the modulation depends on the particular definition of bandwidth employed. Nevertheless, using any reasonable definition of bandwidth, we would expect to be able to achieve, in practice, a spectral efficiency close to (1/2) symbols/s/Hz with this modulation, and, as a result, we shall assume $\eta_F \approx 1/2$ in subsequent analysis.

Another apparent problem with fractal modulation as initially proposed is that it requires infinite transmitter power. Indeed, as Fig. 2 illustrates, $q[n]$ is modulated into an infinite number of octave-width frequency bands. However, in a practical implementation, only a finite collection of contiguous bands $\mathcal{M}$ would, in fact, be used by the transmitter. As a result, the transmitted waveform

$$x(t) = \sum_n q[n] \sum_{m \in \mathcal{M}} \beta^{-m/2} \psi_n^m(t) \tag{37}$$

would exhibit self-similarity only over a range of scales, and demodulation of the data would be possible at one of only a finite number of rates. In terms of Fig. 6, the rate-bandwidth characteristic of the modulation would extend over a finite range of bandwidths chosen to cover extremes anticipated for the system.

The fractal modulation transmitter can be implemented in a computationally highly efficient manner, since much of the processing can be performed using the discrete-time algorithms of Section III-C. For example, synthesizing the waveform $x(t)$ given by (37) for $\mathcal{M} = \{0, 1, \cdots, M-1\}$ involves two states. In the first stage, which involves only discrete-time processing, $q[n]$ is mapped into M consecutive octave-width frequency bands to obtain the sequence $p^{[M]}[n]$. The sequence is obtained using M iterations of the synthesis algorithm (35) with the QMF filter pair $h[n]$, $g[n]$ appropriate to the wavelet basis. The second state then consists of a discrete- to continuous-time transformation in which $p^{[M]}[n]$ is modulated into the continuous-time frequency spectrum via the appropriate scaling function according to

$$\begin{aligned} x(t) &= \sum_n p^{[M]}[n] \phi_n^M(t) \\ &= \sum_n p^{[M]}[n] 2^M \phi(2^M t - n). \end{aligned}$$

It is important to point out that because a batch-iterative algorithm is employed, potentially large amounts of data buffering may be required. Hence, while the algorithm may be computationally efficient, it may be considerably less so in terms of storage requirements. However, in the event that $q[n]$ is *finite length*, it is conceivable that the algorithm may be modified so as to be memory-efficient as well. Such potential remains to be explored.

The transmission of finite length sequences using fractal modulation more generally raises a variety of issues and, therefore, requires some special consideration. In fact, as initially proposed, fractal modulation is rather inefficient in this case, in essence because successively higher frequency band are increasingly underutilized. In particular, we note from the time-frequency portrait in Fig. 2 that if $q[n]$ has finite length, e.g.,

$$q[n] = 0, \qquad n < 0, \quad n > L - 1,$$

then the mth band will complete its transmission of $q[n]$ and go idle in half the time it takes the $(m-1)$st band, and so forth. However, finite length messages may be accommodated rather naturally and efficiently by modulating their periodic extension $q[n \bmod L]$ thereby generating a transmitted waveform

$$x(t) = \sum_n q[n \bmod L] \theta_n^H(t),$$

which constitutes a periodicity-dominated homogeneous signal of the type discussed in Section III-B. If we let

$$\boldsymbol{q} = \{q[0] q[1] \cdots q[L-1]\}$$

denote the data vector, then the time-frequency portrait associated with this signal is shown in Fig. 7. Using this enhancement of fractal modulation, we not only maintain our ability to make various rate-bandwidth tradeoffs at the receiver, but we acquire a certain flexibility in our choice of time origin as

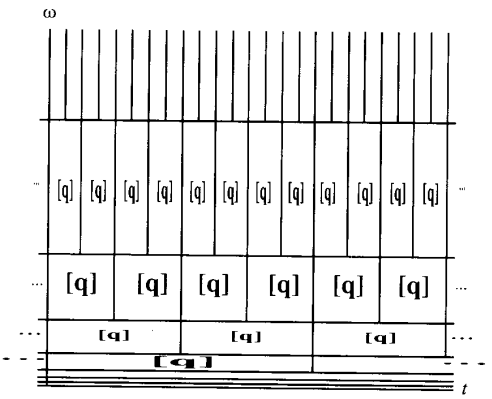

Fig. 7. Portion of the time-frequency portrait of the transmitted signal for fractal modulation of a finite-length data vector q. The case $H = -1/2$ is shown for convenience.

well. Specifically, as is apparent from Fig. 7, the receiver need not begin demodulating the data at $t = 0$, but may more generally choose a time-origin that is some multiple of LR when operating at rate R. Additionally, this strategy can, in principle, be extended to accommodate data transmission on a block-by-block basis.

The final aspect of fractal modulation that remains to be considered in this section concerns the specification of the parameter H. While H has no effect on the spectral efficiency of fractal modulation, it does affect the power efficiency of the scheme. Indeed, it controls the relative power distribution between frequency bands and, hence, the overall transmitted power spectrum, which takes the form (30) where $\gamma = 2H + 1$. Consequently, the selection of H is important when we consider the presence of additive noise in the channel.

For traditional additive stationary Gaussian noise channels of known bandwidth, the appropriate spectral shaping of the transmitted signal is governed by a "water-filling" procedure [11], [12], which is also the method by which the capacity of such channels is computed [13]. Using this procedure, the available signal power is distributed in such a way that proportionally more power is located at frequencies where the noise power is smaller.

When there is uncertainty in the available bandwidth, the water-filling approach leads to poor worst-case performance. As an example, for a channel in which the noise power is very small only in some fixed frequency band $0 < \omega_L < \omega_U < \infty$, the water-filling recipe will locate the signal power predominantly within this band. As a result, the overall SNR in the channel will strongly depend on whether the channel bandwidth is such that these frequencies are passed. By contrast, the distribution of power according to a spectral-matching rule that maintains an SNR that is independent of frequency leads to a system whose performance is uniform with variations in bandwidth and, in addition, is potentially well-suited for LPI communication. Since power-dominated homogeneous signals have a power spectrum of the form of (30), the spectral-matching rule suggests that fractal modulation may be naturally suited to channels with additive $1/f$ noise whose degree H is the same as that of the transmitted signal. This rather broad class of statistically self-similar processes includes not only classical white Gaussian noise ($H = -1/2$) and Brownian motion ($H = 1/2$), but more generally, a range of rather prevalent nonstationary noises which exhibit strong long-term statistical dependence [14].

In this section, we have developed a modulation strategy that satisfies the first of the two system requirements described at the outset of Section IV. In this next section, where we turn our attention to the problem of designing optimal receivers for fractal modulation, we shall see the fractal modulation also satisfies the second of our system requirements.

B. Receiver Design: Demodulation

Consider the problem of recovering a finite length message $q[n]$ from band-limited, time-limited, and noisy observations $r(t)$ of the transmitted waveform $x(t)$ consistent with our channel model of Fig. 5. We shall assume that the noise $z(t)$ is a Gaussian $1/f$ process of degree $H_z = H$, and that the degree H_x of the homogeneous signal $x(t)$ has been chosen according to our spectral-matching rule, i.e.,

$$H_x = H_z = H. \tag{38}$$

We remark that if it is necessary that the transmitter measure H_z in order to perform this spectral matching, the robust and efficient parameter estimation algorithms for $1/f$ processes developed in [7] may be exploited.

Depending on the nature of the message being transmitted, there are a variety of different optimization criteria from which to choose in designing a suitable receiver. As a representative example, we consider the case in which the transmitted message is a random bit stream of length L represented by a binary-valued sequence

$$q[n] \in \{+\sqrt{E_0}, -\sqrt{E_0}\},$$

where E_0 is the energy per bit. For this data, we develop a receiver that demodulates $q[n]$ so as to minimize the probability of a bit-error. Demodulation of non-binary discrete-valued sequences is achieved using a straightforward extension of our results, and demodulation of continuous-valued sequences under a minimum mean-square error criterion is described in [2].

An efficient implementation of the optimum receiver processes the observations $r(t)$ in the wavelet domain by first extracting the wavelet coefficients r_n^m using the DWT (6). These coefficients take the form

$$r_n^m = \beta^{-m/2} q[n \bmod L] + z_n^m, \tag{39}$$

where the z_n^m are the wavelet coefficients of the noise process, and where we have assumed that in accordance with our discussion in Section IV-A the periodic replication of the finite length sequence $q[n]$ has been modulated. To simplify our analysis, we shall further assume that the ideal bandpass wavelet is used in the transmitter and receiver, although we

reiterate that comparable performance can be achieved when more practical wavelets are used.

The duration-bandwidth characteristics of the channel will in general affect which observation coefficients r_n^m may be accessed. In particular, if the channel is bandlimited to 2^{M_U} Hz for some integer M_U, this precludes access to the coefficients at scales corresponding to $m > M_U$. Simultaneously, the duration-constraint in the channel results in a minimum allowable decoding rate of 2^{M_L} symbols/sec for some integer M_L, which precludes access to the coefficients at sales corresponding to $m < M_L$. As a result, the collection of coefficients available at the receiver is

$$r = \{r_n^m,\ m \in \mathcal{M},\ n \in \mathcal{N}(m)\},$$

where

$$\mathcal{M} = \{M_L,\ M_L + 1, \cdots, M_U\},$$
$$\mathcal{N}(m) = \{0, 1, \cdots, L2^{m-M_L} - 1\}.$$

This means that we have available

$$K = \sum_{m=M_L}^{M_U} 2^{m-M_L} = 2^{M_U - M_L + 1} - 1 \tag{40}$$

noisy measurements of each of the L nonzero samples of the sequence $q[n]$. The specific relationship between decoding rate R, bandwidth W, and redundancy K can, therefore, be expressed in terms of the spectral efficiency of the modulation η_F as

$$\frac{R}{W} = \frac{2\eta_F}{K+1}, \tag{41}$$

where, as discussed earlier, $\eta_F \approx 1/2$. Note that $M_U = M_L$ when $K = 1$, and (41) attains its maximum value, η_F.

The optimal decoding of each bit can be described in terms of a binary hypothesis test on the set of available observation coefficients r. Denoting by H_1 the hypothesis in which $q[n] = +\sqrt{E_0}$, and by H_0 the hypothesis in which $q[n] = -\sqrt{E_0}$, we may construct the likelihood ratio test for the optimal decoding of each symbol $q[n]$. The derivation is particularly straightforward because of the fact that, in accordance with the wavelet-based models for $1/f$ processes developed in [15], [7], [2], the z_n^m in (39) may be modeled as independent zero-mean Gaussian random variables with variances

$$\text{var } z_n^m = \sigma_z^2 \beta^{-m}, \tag{42}$$

for some variance parameter $\sigma_z^2 > 0$. Consequently, the likelihood ratio test reduces to the test

$$l = \sum_{m=M_L}^{M_U} \sum_{l=0}^{2^{m-M_L}-1} \frac{r_{n+lK}^m \cdot \sqrt{E_0}\,\beta^{-m/2}}{\sigma_z^2 \beta^{-m}} \underset{H_0}{\overset{H_1}{\gtrless}} 0$$

under the assumption of equally likely hypotheses, i.e., a random bit stream. The bit-error probability associated with this optimal receiver is, of course, readily derived, and can be expressed as

$$\Pr(\epsilon) = \Pr(l > 0 \mid H_0) = Q\left(\frac{1}{2}\sqrt{K\sigma_c^2}\right), \tag{43}$$

where $Q(\cdot)$ is defined by

$$Q(x) = \frac{1}{\sqrt{2\pi}} \int_x^\infty e^{-v^2/2}\, dv,$$

and where σ_c^2 is the SNR in the channel, i.e.,

$$\sigma_c^2 = \frac{E_0}{\sigma_z^2}.$$

Substituting for K in (43) via (41) we can rewrite this error probability in terms of the channel rate-bandwidth ratio as

$$\Pr(\epsilon) = Q\left(\frac{1}{2}\sqrt{\sigma_c^2\left[\frac{2\eta_F}{R/W} - 1\right]}\right), \tag{44}$$

where, again, $\eta_F \approx 1/2$. Note that the performance of fractal modulation is independent of the spectral exponent of the noise process when we use spectral matching.

To establish a performance baseline, we shall also evaluate a modified version of our benchmark modulation in which we incorporate repetition-coding, i.e., in which we add redundancy by transmitting each sample of the message sequence K times in succession. This comparison scheme is not particularly power efficient both because signal power is distributed uniformly over the available bandwidth irrespective of the noise spectrum, and because much more effective redundancy schemes can be used with channels of known bandwidth (see, e.g., [16]). Nevertheless, with these caveats in mind, such comparisons do lend some insight into the *relative* power efficiency of fractal modulation.

In our modified benchmark modulation, incorporating redundancy reduces the effective decoding rate per unit bandwidth by a factor of K, i.e.,

$$\frac{R}{W} = \frac{\eta_0}{K}, \tag{45}$$

where η_0 is the efficiency of the modulation without coding, i.e., unity. When the channel adds stationary white Gaussian noise, for which $H = -1/2$, the optimum receiver for this scheme demodulates the received data and averages together the K symbols associated with the transmitted bit, thereby generating a sufficient statistic. When this statistic is positive the receiver decodes a 1-bit, and a 0-bit otherwise. The corresponding performance is, therefore, given by

$$\Pr(\epsilon) = Q\left(\frac{1}{2}\sqrt{\sigma_c^2 K}\right) = Q\left(\frac{1}{2}\sqrt{\sigma_c^2\left[\frac{\eta_0}{R/W}\right]}\right), \tag{46}$$

where the last equality results from substituting for K via (45).

Comparing (46) with (44), we note that since $\eta_0 \approx 2\eta_F$, the asymptotic bit-error performances of fractal modulation and the benchmark scheme are effectively equivalent for $R/W \ll \eta_F$, as is illustrated in Fig. 8. In Fig. 8(a), $\Pr(\epsilon)$ is

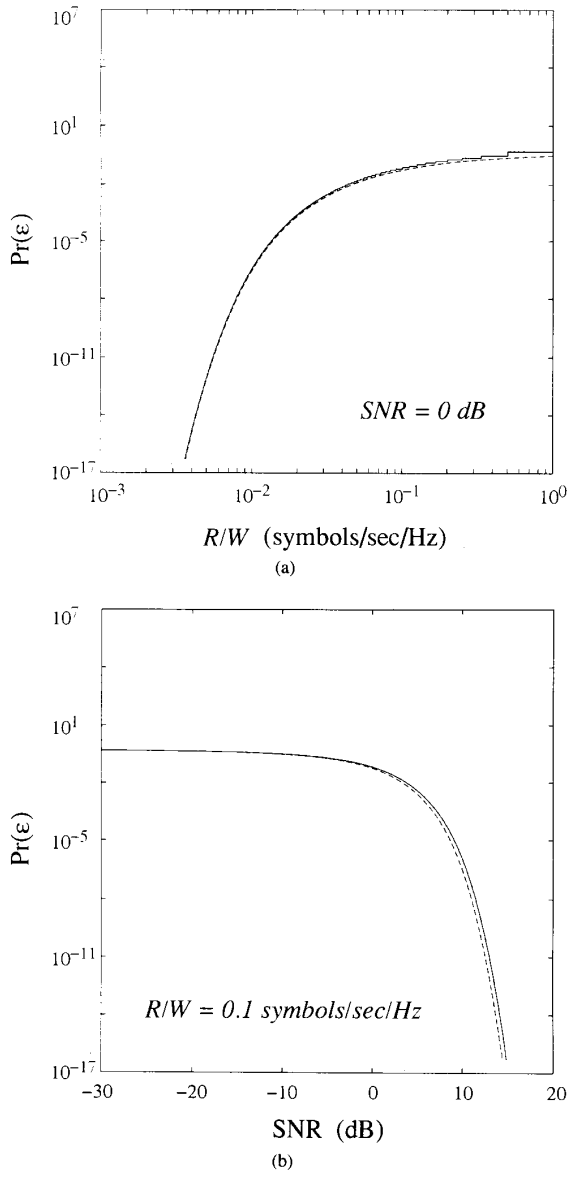

Fig. 8. Bit-error rate performance of fractal modulation. (a) $\Pr(\epsilon)$ as a function of rate/bandwidth ratio R/W at 0 dB SNR. (b) $\Pr(\epsilon)$ as a function of SNR at $R/W = 0.1$ symbols/s/Hz. Solid lines indicate the performance of fractal modulation, while dashed lines indicate the performance of the benchmark modulation with repetition coding.

shown as a function of R/W at a fixed SNR of 0 dB ($\sigma_c^2 = 1$), while in Fig. 8(b), $\Pr(\epsilon)$ is shown as a function of SNR at a fixed $R/W = 0.1$ bits/s/Hz. Both these plots reveal strong thresholding behavior whereby the error probability falls off dramatically at high SNR and low R/W. We emphasize that comparisons between the two schemes are appropriate only for the case in which the noise has parameter $H = -1/2$, corresponding to the case of stationary white Gaussian noise. For other values of H, the performance of the benchmark modulation is not only difficult to evaluate, but necessarily poor as well because of inefficient distribution of power among frequencies.

V. Concluding Comments

We have developed convenient, efficient, and robust wavelet-based representations for a generalized class of homogeneous signals, and explored their properties. Furthermore, we have explored their potential for use as modulating waveforms in a communications-based application, and demonstrated that fractal modulation would appear to be well-suited for use with noisy channels of simultaneously uncertain duration and bandwidth.

While our development of fractal modulation considered many issues, many others, such as synchronization and buffering, remain to be investigated. Furthermore, there are many potential refinements to be explored. One might involve the incorporation of block or trellis coding techniques to improve the power efficiency of the modulation. It would seem that coding of this type cannot be incorporated without sacrificing properties of the transmission scheme. In particular, the simple redundancy scheme apparent in Fig. 7 enables the recovery of a message $\boldsymbol{q}$ from observations corresponding to *any* single cell of the time-frequency plane. Nevertheless, it would be important to identify the trade-offs involved.

The potential of fractal modulation in LPI applications also remains to be explored. While we have argued that the second-order statistics of homogeneous signals are effectively indistinguishable from those of $1/f$ noises, a more comprehensive study of the detectability of homogeneous signals is warranted. In the process, some potentially useful extensions to fractal modulation may arise. As an example, drawing from the notions underlying direct-sequence spread spectrum, one technique for more effectively concealing the modulation from unintended receivers might involve premultiplying the entire wavelet coefficient field x_n^m of the signal $x(t)$ prior to transmission by a pseudorandom bit field known to both transmitter and receiver.

Finally, we remark that there would appear to be many additional applications for the self-similar signals we have introduced in this paper. In many respects, identifying and exploring other potentially promising applications represents perhaps the most exciting direction for future research.

Acknowledgment

The authors wish to thank Prof. A. S. Willsky for many valuable discussions, comments and suggestions regarding this work. They also wish to thank the anonymous reviewers for their careful reading and thoughtful criticisms of the original manuscript, which led to significant improvements in the presentation of this work.

Appendix A

Proof of Theorem 1

To show that $y(t)$ has finite energy, we exploit an equivalent synthesis for $y(t)$ as the output of a cascade of filters driven by $x(t)$, the first of which is an ideal bandpass filter whose passband

includes $\omega_L < |\omega| < \omega_U$, and the second of which is the filter given by (10).

Let $b_m(t)$ be the impulse response of a filter whose frequency response is given by

$$B_m(\omega) = \begin{cases} 1, & 2^m\pi < |\omega| \le 2^{m+1}\pi, \\ 0, & \text{otherwise}, \end{cases} \tag{47}$$

and let $b(t)$ be the impulse response corresponding to (10). Furthermore, choose finite integers M_L and M_U such that $2^{M_L}\pi < \omega_L$ and $\omega_U < 2^{M_U+1}\pi$. Then using the asterisk to denote convolution,

$$\begin{aligned} y(t) &= b(t) * \left[\sum_{m=M_L}^{M_U} b_m(t) \right] * x(t) \\ &= b(t) * \sum_{m=M_L}^{M_U} \tilde{x}_m(t), \end{aligned} \tag{48}$$

where

$$\tilde{x}_m(t) = x(t) * b_m(t) = 2^{-mH}\tilde{x}_0(2^m t), \tag{49}$$

and where the last equality in (49) results from an application of the self-similarity relation (8) and the identity

$$b_m(t) = 2^m b_0(2^m t).$$

Because $x(t)$ is energy-dominated, $\tilde{x}_0(t)$ has finite energy. Hence, (49) implies that every $\tilde{x}_m(t)$ has finite energy. Exploiting this fact in (48) allows us to conclude that $y(t)$ must have finite energy as well.

To verify the spectrum relation (11), we express (48) in the Fourier domain. Exploiting the fact that we may arbitrarily extend the limits in the summation in (48), we get

$$\begin{aligned} Y(\omega) = B(\omega) \sum_{m=-\infty}^{\infty} \tilde{X}_m(\omega) \\ = \begin{cases} X(\omega), & \omega_L < |\omega| < \omega_U, \\ 0, & \text{otherwise}, \end{cases} \end{aligned}$$

where $\tilde{X}_m(\omega)$ denotes the Fourier transform of $\tilde{x}_m(t)$, and where

$$X(\omega) \triangleq \sum_{m=-\infty}^{\infty} \tilde{X}_m(\omega). \tag{50}$$

The right-hand side of (50) is, of course, pointwise convergent because for each ω at most one term in the sum is nonzero. Finally, exploiting (49) in (50) gives

$$X(\omega) = \sum_m 2^{-m(H+1)}\tilde{X}_0(2^{-m}\omega),$$

which, as one can readily verify, satisfies (12).

Appendix B

Proof of Theorem 2

To prove the "only if" statement, we suppose $x(t) \in E^H$ and being by expressing $x(t)$ in terms of the ideal bandpass wavelet basis $\{\tilde{\psi}_n^m(t)\}$. In particular, we let

$$x(t) = \sum_m \tilde{x}_m(t),$$

where

$$\tilde{x}_m(t) = \beta^{-m/2} \sum_n \tilde{q}[n]\tilde{\psi}_n^m(t)$$

and where $\tilde{q}[n]$, the generating sequence in this basis, has energy $\tilde{E} < \infty$. The new generating sequence $q[n]$ can then be expressed as

$$q[n] = \sum_m q_m[n], \tag{51}$$

where

$$q_m[n] = y_m(t)\,|_{t=n}$$

and

$$y_m(t) = \tilde{x}_m(t) * \psi(-t).$$

For each m, since $\tilde{x}_m(t)$ is bandlimited, $y_m(t)$ and $q_m[n]$ each have finite energy and Fourier transforms $Y_m(\omega)$ and $Q_m(\omega)$, respectively. Hence,

$$Q_m(\omega) = \sum_k Y_m(\omega - 2\pi k), \tag{52}$$

where

$$\begin{aligned} &Y_m(\omega) \\ &= \begin{cases} (2\beta)^{-m/2}\Psi^*(\omega)\tilde{Q}(2^{-m}\omega), & 2^m\pi < |\omega| \le 2^{m+1}\pi, \\ 0, & \text{otherwise}, \end{cases} \end{aligned}$$

with $\tilde{Q}(\omega)$ denoting the Fourier transform of $\tilde{q}[n]$, and $\Psi^*(\omega)$ the complex conjugate of $\Psi(\omega)$.

In deriving bounds on the energy E_m in each sequence $q_m[n]$ for a fixed m, it is convenient to consider the cases $m \le -1$ and $m \ge 0$ separately. When $m \le -1$, the sampling by which $q_m[n]$ is obtained involves no aliasing. Since on $|\omega| \le \pi$ we then have

$$Q_m(\omega) = Y_m(\omega),$$

we may deduce that $q_m[n]$ has energy

$$\begin{aligned} E_m &= \sum_n |q_m[n]|^2 \\ &= \frac{(2\beta)^{-m}}{\pi} \int_{2^m\pi}^{2^{m+1}\pi} |\Psi(\omega)|^2 |\tilde{Q}(2^{-m}\omega)|^2 \, d\omega. \end{aligned} \tag{53}$$

Because $\psi(t)$ has R vanishing moments, there exists a $0 < \epsilon_0 < \infty$ such that

$$|\Psi(\omega)| \le \epsilon_0 |\omega|^R, \tag{54}$$

for all ω. Exploiting this in (53) we obtain

$$E_m \le C_0 2^{(2R-\gamma)m}\tilde{E}, \tag{55}$$

for some $0 \le C_0 < \infty$.

Consider, next, the case corresponding to $m \ge 0$. Since $\psi(t)$ has R vanishing moments, there also exists a $0 < \epsilon_1 < \infty$ such that

$$|\Psi(\omega)| \le \epsilon_1 |\omega|^{-R} \tag{56}$$

for all ω. Hence, on $2^m\pi < |\omega| \le 2^{m+1}\pi$,

$$|Y_m(\omega)| \le \epsilon_1 \pi^{-R} 2^{-(\gamma+1+2R)m/2} |\tilde{Q}(2^{-m}\omega)|. \tag{57}$$

From (52), we obtain

$$\begin{aligned} |Q_m(\omega)| &\le \epsilon_1 \pi^{-R} 2^{-(\gamma+1+2R)m/2} \\ &\quad \cdot \sum_{k=0}^{2^m-1} |\tilde{Q}(2^{-m}\omega + 2\pi k 2^{-m})| \end{aligned} \tag{58}$$

by exploiting, in order, the triangle inequality, the bound (57), the fact that only 2^m terms in the summation in (52) are nonzero since $y_m(t)$ is bandlimited, and the fact that $\tilde{Q}(\omega)$ is 2π-periodic. In turn, we may use, in order, (58), the Schwarz inequality, and again the

periodicity of $\tilde{Q}(\omega)$ to conclude that

$$E_m \le \epsilon_1^2 \pi^{-2R} 2^{-(\gamma+1+2R)m} \cdot \left[\sum_{k=0}^{2^m-1} \sqrt{\frac{1}{2\pi} \int_{-\pi}^{\pi} |\tilde{Q}(2^{-m}\omega + 2\pi k 2^{-m})|^2 \, d\omega} \right]^2 \le C_1 2^{-(\gamma-2+2R)m} \tilde{E}, \quad (59)$$

for some $0 \le C_1 < \infty$.

Using (51), the triangle inequality, and the Schwarz inequality, we obtain the following bound on the energy in $q[n]$

$$E = \sum_n |q[n]|^2 \le \left[\sum_m \sqrt{E_m} \right]^2$$

which, from (59) and (55) is finite provided $0 < \gamma < 2R$ and $R \ge 1$.

Let us now show the converse. Suppose $q[n]$ has energy $E < \infty$, and express $x(t)$ as

$$x(t) = \sum_m x_m(t),$$

where

$$x_m(t) = \beta^{-m/2} \sum_n q[n] \psi_n^m(t).$$

If we let

$$\tilde{y}_m(t) = b_0(t) * x_m(t),$$

where $b_0(t)$ is the impulse response of the ideal bandpass filter (9), it suffices to show that

$$\tilde{y}(t) = \sum_m \tilde{y}_m(t) \quad (60)$$

has finite energy.

For each m, we begin by bounding the energy in $\tilde{y}_m(t)$, which is finite because $x_m(t)$ has finite energy. Since $\tilde{y}_m(t)$ has Fourier transform

$$\tilde{Y}_m(\omega) = \begin{cases} (2\beta)^{-m/2} Q(2^{-m}\omega) \Psi(2^{-m}\omega), & \pi < |\omega| < 2\pi, \\ 0, & \text{otherwise} \end{cases}$$

where $Q(\omega)$ is the discrete-time Fourier transform of $q[n]$, we get that

$$\tilde{E}_m = \frac{2^{-\gamma m}}{\pi} \int_{2^{-m}\pi}^{2^{-m+1}\pi} |Q(\omega)|^2 |\Psi(2^{-m}\omega)|^2 \, d\omega.$$

Again, it is convenient to consider the cases corresponding to $m \le -1$ and $m \ge 0$ separately. For $m \le -1$, most of the energy in $x_m(t)$ is at frequencies below the passband of the bandpass filter. Hence, using the bound (56) and exploiting the periodicity of $Q(\omega)$ we obtain

$$\tilde{E}_m \le \tilde{C}_0 2^{(2R-1-\gamma)m} E, \quad (61)$$

for some $0 \le \tilde{C}_0 < \infty$. For $m \ge 0$, most of the energy in $x_m(t)$ is at frequencies higher than the passband of the bandpass filter. Hence, using the bound (54) we obtain

$$\tilde{E}_m \le \tilde{C}_1 2^{-(\gamma+2R+1)m} E, \quad (62)$$

for some $0 \le \tilde{C}_1 < \infty$.

Finally, using (60), the triangle inequality, and the Schwarz inequality, we obtain the following bound on the energy in $\tilde{y}(t)$

$$\tilde{E} = \int_{-\infty}^{\infty} |\tilde{y}(t)|^2 \, dt \le \left[\sum_m \sqrt{\tilde{E}_m} \right]^2,$$

which, from (62) and (61) is finite provided $0 < \gamma < 2R - 1$ since $R \ge 1$.

Appendix C

Proof of Theorem 3

Following an approach analogous to the proof of Theorem 1, let $b_m(t)$ be the impulse response of a filter whose frequency response is given by (47), and let $b(t)$ be the impulse response corresponding to (10). By choosing finite integers M_L and M_U such that $2^{M_L}\pi < \omega_L$ and $\omega_U < 2^{M_U+1}\pi$, we can again express $y(t)$ in the form of (48). Because $x(t)$ is power-dominated, $\tilde{x}_0(t)$ has finite power. Hence, (49) implies that every $\tilde{x}_m(t)$ has finite power. Exploiting this fact in (48) allows us to conclude that $y(t)$ must have finite power as well.

To verify the spectrum relation (28), we use (48) together with the fact that the $\tilde{x}_m(t)$ are uncorrelated for different m to obtain

$$S_y(\omega) = |B(\omega)|^2 \sum_{m=-\infty}^{\infty} S_{\tilde{x}_m}(\omega) = \begin{cases} S_x(\omega), & \omega_L < |\omega| < \omega_U, \\ 0, & \text{otherwise} \end{cases}$$

where $S_{\tilde{x}_m}(\omega)$ denotes the power spectrum of $\tilde{x}_m(t)$, and where

$$S_x(\omega) \triangleq \sum_{m=-\infty}^{\infty} S_{\tilde{x}_m}(\omega). \quad (63)$$

Again we have exploited the fact that the upper and lower limits on the summation in (48) may be extended to ∞ and $-\infty$, respectively. The right-hand side of (63) is, again, pointwise convergent because for each ω at most one term in the sum is nonzero. Finally, exploiting (49) in (63) gives

$$S_x(\omega) = \sum_m 2^{-\gamma m} S_{\tilde{x}_0}(2^{-m}\omega)$$

which, as one can readily verify, satisfies (29).

References

[1] I. M. Gel'fand, G. E. Shilov, N. Y. Vilenkin, and M. I. Graev, *Generalized Functions*. New York: Academic Press, 1964.

[2] G. W. Wornell, "Synthesis, analysis, and processing of fractal signals," RLE tech. rep. No. 566, M.I.T., Cambridge, MA, Oct. 1991.

[3] S. G. Mallat, "A theory for multiresolution signal decomposition: The wavelet representation," *IEEE Trans. Pattern Anal. Machine Intell.*, vol. PAMI-11, pp. 674-693, July 1989.

[4] I. Daubechies, "Orthonormal bases of compactly supported wavelets," *Commun. Pure Appl. Math.*, vol. 41, pp. 909-996, Nov. 1988.

[5] B. B. Mandelbrot, *The Fractal Geometry of Nature*. San Francisco, CA: Freeman, 1982.

[6] P. Flandrin, "On the spectrum of fractional Brownian motions," *IEEE Trans. Inform. Theory*, vol. 35, pp. 197-199, Jan. 1989.

[7] G. W. Wornell and A. V. Oppenheim, "Estimation of fractal signal from noisy measurements using wavelets," to appear in *IEEE Trans. Signal Processing*, 1992.
[8] G. Strang, "Wavelets and dilation equations: A brief introduction," *SIAM Rev.*, vol. 31, pp. 614-627, Dec. 1989.
[9] M. F. Bransley, *Fractals Everywhere*. New York: Academic Press, 1988.
[10] F. J. Malassenet and R. M. Mersereau, "Wavelet representations and coding of self-affine signals," in *Proc. Int. Conf. Acoust. Speech, Signal Processing*, Toronto, ON, Canada, May 1991, pp. 677-680.
[11] J. A. C. Bingham, "Multicarrier modulation for data transmission: An idea whose time has come," *IEEE Comm. Mag.*, pp. 5-14, May 1990.
[12] I. Kalet, "The multitone channel," *IEEE Trans. Commun.*, vol. 37, p. 119-124, Feb. 1989.
[13] R. G. Gallager, *Information Theory and Reliable Communication*. New York: John Wiley, 1968.
[14] M. S. Keshner, "$1/f$ noise," *Proc. IEEE*, vol. 70 pp. 212-218, Mar. 1982.
[15] G. W. Wornell, "A Karhunen-Loève-like expansion for $1/f$ processes via wavelets," *IEEE Trans. Inform. Theory*, vol. 36, p. 859-861, July 1990.
[16] G. D. Forney, Jr., R. G. Gallager, G. R. Lang, F. M. Longstaff, and S. U. Qureshi, "Efficient modulation for band-limited channels," *IEEE J. Select. Areas Commun.*, vol. SAC-2, pp. 632-647, Sept. 1984.